*t*BuP(NH$_2$)$_2$—A Reactive Synthon for the Synthesis of Molecular Imidophosphinates of Group 13 Metals

T. Bauer,[a] S. Schulz,*[a] M. Nieger,[a] and I. Krossing*[b]

Abstract: Reactions of *t*BuP(NH$_2$)$_2$ with Group 13 trialkyls MR$_3$ (M = Al, Ga, In; R = Me, *t*Bu) were investigated in detail. According to variable-temperature (VT) NMR investigations, the reaction proceeds stepwise with the initial formation of aminophosphane adducts, which subsequently react to give iminophosphorane adducts and finally the heterocyclic metallonitridophosphinates. BP86/TZVPP (DFT) calculations were performed to verify this reaction pathway, to elucidate the influence of the central Group 13 element on the stability of the reaction intermediates and the heterocycles, as well as to assess the thermodynamics of their formation. The relative stability of free and complexed aminophosphane RP(NH$_2$)$_2$ and iminophosphorane R(H$_2$N)(H)P=NH (adducts) with P^{III} and P^{V} centers was studied in more detail with DFT and MP2 methods. In addition, the influence of the substituent R was investigated by variation of R from H to Me, *t*Bu, F, and NH$_2$. In general, the aminophosphane form was found to be favored for the free ligand, however, upon complexation with MR$_3$ (M = Al, Ga; R = alkyl) both forms are almost equal in energy.

Keywords: ab initio calculations · density functional calculations · donor–acceptor systems · Group 13 elements · main group elements · phosphorus

Introduction

The synthesis and reactivity of (dialkylamino)phosphanes of the type R$_x$P(NR'$_2$)$_{3-x}$ (R, R' = alkyl, aryl; $x = 0$–2), which have been known for more than a century,[1] has been studied in detail. The presence of both hard (N) and soft (P) Lewis basic centers (HSAB principle) renders them very interesting for coordination chemistry. In contrast, (alkylamino)phosphanes R$_x$P(NHR')$_{3-x}$ ($x = 0$,[2] 1,[3] 2[4]) and aminophosphanes R$_x$P(NH$_2$)$_{3-x}$ ($x = 1$,[5] 2[6]) have been investigated to a much lesser extent. Compared to the NR$_2$-substituted derivatives, their stability is significantly reduced both in solution and in their pure form. Consecutive condensation reactions leading to the formation of cyclic or oligomeric phosphazanes is favored in the compounds containing an increasing number of amino groups and decreasing steric demand of the organic substituents (R, R'). Consequently, trisaminophosphane P(NH$_2$)$_3$ has only been isolated as BH$_3$[7] and metal carbonyl complexes,[8] to date.[9] In addition, only a single bis(amino)phosphane (*t*BuP(NH$_2$)$_2$) has been synthesized and characterized.[5,6]

We became interested in aminophosphanes due to their potential capability for the generation of Group 13/15 compounds containing an M-N-P backbone (M = Al, Ga, In). The reaction of (Cy$_2$N)$_2$PNH$_2$ with trialkyl- and dialkylalanes proceeds with adduct formation to give (Cy$_2$N)$_2$P(H)N(H)−AlR$_3$ (**I**) or with H$_2$ elimination and subsequent formation of dimeric heterocycles [{(Cy$_2$N)$_2$P(H)NAlR$_2$}$_2$] (**II**; Scheme 1).[10]

Both **I** and **II** adopt the iminophosphorane form (P(H) form **IV**) which is thermodynamically favored over the corresponding aminophosphane structure (N(H) form **V**). In contrast, *t*BuP(NH*t*Bu)$_2$ reacts with Group 13 metal organic compounds (AlH$_3$−NMe$_3$, R$_2$AlH, MR$_3$ (M = Al, Ga, In)) with preservation of the N(H) form.[11] The equilibrium (Scheme 2) between the aminophosphane and iminophosphorane form is known to depend on the electronic properties of the ligands bound to the N and the P center[12] as was confirmed by computational calculations on the free R$_2$P−N(H)$^-$ (N(H) form **V**) and R$_2$P(H)=N$^-$ (P(H) form **IV**) anions (R = H, NH$_2$ and NMe$_2$) as well as neutral Group 4 complexes.[13]

Consequently, we became interested in reactions of bisaminophosphanes RP(NH$_2$)$_2$ and Group 13 metal organic

---

[a] Dipl.-Chem. T. Bauer, Priv.-Doz. Dr. S. Schulz, Dr. M. Nieger
Institut für Anorganische Chemie der Universität Bonn
Gerhard-Domagk-Strasse 1, 53121 Bonn (Germany)
Fax: (+49) 228-735327
E-mail: sschulz@uni-bonn.de

[b] Priv.-Doz. Dr. I. Krossing
Institut für Anorganische Chemie, Universität Karlsruhe
Engesserstr Geb 30–45, 76128 Karlsruhe (Germany)
Fax: (+49) 721-6084854
E-mail: krossing@chemie.uni-karlsruhe.de

Supporting information for this article is available on the WWW under http://www.chemeurj.org/ or from the author.

DOI: 10.1002/chem.200305530

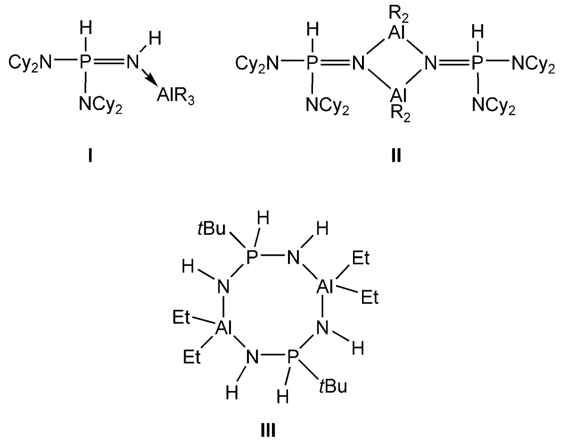

Scheme 1. Reaction products **I–III** previously obtained from the reactions of aminophosphanes with organoaluminum compounds.

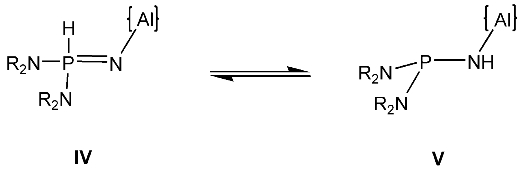

Scheme 2. P(H) (**IV**) and N(H) (**V**) tautomeric forms of aminophosphanes.

compounds. To our surprise, the reaction of $t\mathrm{BuP(NH_2)_2}$ with $\mathrm{Et_2AlH}$ yielded the eight-membered heterocycle $[\{t\mathrm{Bu(H)P(NH)_2AlEt_2}\}_2]$ (**III**; Scheme 1).[14] Heterocycle **III** represents the first structurally characterized aluminonitridophosphinate. Its central structural motif is represented by an eight-membered ring, containing two P, two Al, and four N centers. Comparable structural units have been previously observed for isoelectronic Group 13 phosphinates (replacement of a NH group by an isoelectronic oxygen atom), which were prepared by reactions of $\mathrm{MR_3}$ with phosphinic acid $\mathrm{R_2P(O)OH}$, and for Group 13 phosphonates and phosphates.[15] Such compounds are of interest due to their potential conversion into microporous materials with promising applications as molecular sieves or in catalysis. The electronic and structural similarity between imido and oxo anions, which has been subject to several studies within the last decade, renders Group 13 nitridophosphinates, -phosphonates, and phosphates very interesting synthetic goals.[16] Herein we report on the reactions of $t\mathrm{BuP(NH_2)_2}$ with Group 13 element trialkyls $\mathrm{MMe_3}$ (M = Al, Ga, In) and $\mathrm{M}t\mathrm{Bu_3}$ (M = Al, Ga). Quantum-chemical calculations were performed to verify the proposed reaction pathway and to gain a detailed understanding on the stability of possible reaction intermediates.

Results and Discussion

Quantum-chemical calculations I: It is known for $t\mathrm{BuP(NH_2)_2}$ that the N(H) form is thermodynamically favored over the P(H) form, whereas for the corresponding OH-substituted derivative the P(H) form (tBu(H)P(O)OH) is preferred.[17] To investigate the influence of both steric and electronic properties of the ligand R on the relative stability of the N(H) form ($\mathrm{RP(NH_2)_2}$) and P(H) form ($\mathrm{R(H)(NH_2)P{=}NH}$), the relative energies $E_{\mathrm{rel.}}$ for both tautomers were investigated for R = H, $\mathrm{CH_3}$, tBu, F, and $\mathrm{NH_2}$ by BP86/SV(P) and MP2/TZVPP [in brackets] (see Table 1).

Table 1. The relative energies $E_{\mathrm{rel.}}$ [kJ mol^{-1}] of the aminophosphane (NH) and iminophosphorane (PH) form of $\mathrm{RP(NH_2)_2}$ at the BP86/SV(P) level (MP2/TZVPP). P–N bond lengths in both forms are given in pm [MP2/TZVPP values].

R	$E_{\mathrm{rel.}}$(NH)	$E_{\mathrm{rel.}}$(PH)	d(P–N) (NH)	d(P–N) (PH)
F	0 (0)	70 (44)	169	154/166
$\mathrm{NH_2}$	0 (0)	58 (35)	172	156/168/169
H	0 (0)	101 (75)	171	156/168
$\mathrm{CH_3}$	0 (0)	83 (61)	172	156/169
$\mathrm{C(CH_3)_3}$	0 (0)	78 (63)	172	157/168

In agreement with the experiment, the calculations for $t\mathrm{BuP(NH_2)_2}$ showed the N(H) form to be more stable than the P(H) form by 78 [63] kJ mol^{-1}. These findings clearly demonstrate that the equilibrium between the N(H) and the P(H) form lies on the $t\mathrm{BuP(NH_2)_2}$ side prior to the addition of the Group 13 trialkyl. Changing R from tBu to H leads to a slight increase of the stability of the N(H) form by 23 [12] kJ mol^{-1}. If R is changed from tBu to more electronegative $\mathrm{NH_2}$ or F, the N(H) form is still the most favored minimum but only stabilized by 58 [35] kJ mol^{-1} ($\mathrm{NH_2}$) and 70 [44] kJ mol^{-1} (F), respectively. In addition, electronegative substituents also lead to gradually shorter P–N bonds.

Reactions of tBuP(NH$_2$)$_2$ with MMe$_3$: Reactions of $t\mathrm{BuP(NH_2)_2}$ with $\mathrm{MMe_3}$ (M = Al, Ga, In) between −78 and +25 °C proceed with a smooth gas evolution and the formation of eight-membered heterocycles $[\{t\mathrm{Bu(H)P(NH)_2MMe_2}\}_2]$ (M = Al **1**, Ga **2**, In **3**; [Eq. (1)].

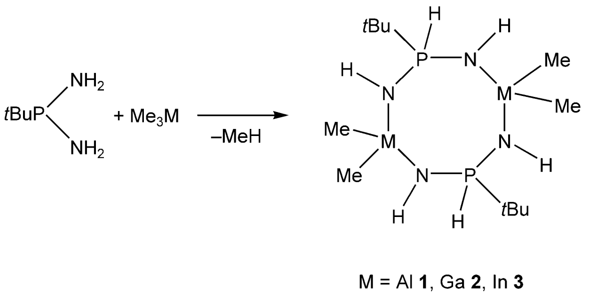

(1)

^{31}P NMR spectra of **1** and **2** each show two well-separated resonances with different intensities (δ = 46.0, 46.7 ppm (65:35) **1**; δ = 46.5, 47.3 ppm (60:40) **2**), whereas those of **3** (δ = 51.4 ppm) overlap. This indicates the presence of two different isomers of the corresponding eight-membered heterocycles in solution as was previously observed for the reaction with $\mathrm{Et_2AlH}$.[14] Consequently, ^{1}H and ^{13}C NMR spectra of **1**, **2**, and **3** also show two sets of resonances due to the organic ligands (Me, *t*Bu, H). Intense vibrational bands at typical positions for N–H and P–H moieties in the IR spectra clearly prove the formation of the P(H) iminophosphoran form. Compounds **1**, **2**, and **3** are fairly stable in the gas phase as is indicated by their mass spectra, which show peaks for the molecular ion $[M]^+$ (**1**) or for the fragments $[M{-}\mathrm{Me}]^+$ (**2**, **3**).

Suitable single crystals for an X-ray structure determination were slowly grown from a solution of **1** in hexane at −30 °C (Figure 1). ^{31}P NMR spectra of as-formed crystals almost exclusively show resonances due to the *trans* isomer, whereas only very small quantities of the *cis* isomer are present (98:2). In contrast, several attempts to obtain single crystals of **2** and **3** failed. The presence of almost equimolar quantities of both the *cis* and *trans* isomer probably prevents samples of **2** and **3** from growing X-ray quality crystals.

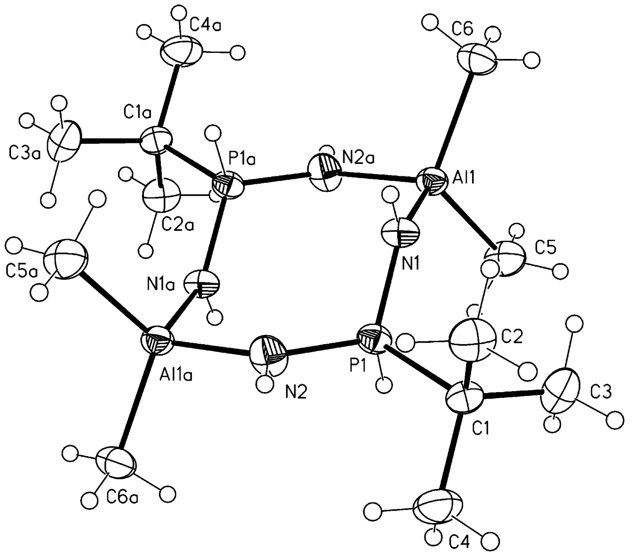

Figure 1. ORTEP diagram (50 % probability ellipsoids) showing the solid-state structure and atom-numbering scheme of **1**. Selected bond lengths [Å] and angles [°]: P1–N1 1.612(2), P1–N2 1.603(2), P1–C1 1.831(2), P1–H1P 1.397(14), Al1–N1 1.882(2), Al1–N2#1 1.893(2), Al1–C5 1.971(2), Al1–C6 1.977(2), N1-H1N 0.860(15); N1-P1-N2 115.6(1), N2-P1-C1 109.7(1), N1-P1-C1 112.4(1), N1-Al1-N2#1 103.0(1), N1-Al1-C5 112.0(1), N2#1-Al1-C5 108.2(1), C5-Al1-C6 118.1(1), P1-N1-Al1 132.5(1), P1-N2-Al1#1 127.6(1).

Compound **1** crystallizes in the monoclinic space group $P2_1/c$ (no. 14). Its central structural parameters are very similar to those of $[\{t\mathrm{Bu(H)P(NH)_2AlEt_2}\}_2]$. The eight-membered ring shown in Figure 1 adopts a chairlike conformation with the P and Al centers in a (distorted) tetrahedral environment and the *t*Bu groups in a transoid orientation. The three-coordinate N centers are almost planar as is reflected by their sums of the bond angles (359.6° N1, 359.2° N2). The endocyclic P-N-Al bond angles (132.5(1), 127.6(1)°) are significantly larger than the N-P-N (115.6(1)°) and N-Al-N angles (103.0(1)°). Analogous structural findings were observed for $[\{t\mathrm{Bu(H)P(NH)_2AlEt_2}\}_2]$ and aluminophosphinates $[\mathrm{R(H)P(O)_2AlR_2}]_2$. The exocyclic C-Al-C and C-P-H bond angles are 118.1(1)° and 103.8(7)°, respectively. The Al–N distances range from 1.882(2) to 1.893(2) Å, as is typical for four-coordinate Al and three-coordinate N centers. The P–N bond lengths (1.603(2), 1.612(2) Å) clearly indicate the π-bonding character within the $\mathrm{PN_2}$ fragment. The Al–C (1.971(2), 1.977(2) Å), N–H (0.86(2), 0.83(2) Å), P–H (1.40(2) Å), and P–C bond lengths (1.831(2) Å) as observed in **1** are within expected ranges.

In an attempt to get some insight on the reaction pathway leading to the formation of **1**–**3**, variable-temperature ^{1}H and ^{31}P NMR studies were performed (Figure 2).

The low-temperature ^{31}P NMR spectrum (−80 °C) of the reaction of $t\mathrm{BuP(NH_2)_2}$ with $\mathrm{AlMe_3}$ shows a signal of the starting bisaminophosphane ($\delta = 58.5$ ppm) and a singlet at $\delta = 93.3$ ppm, which most likely indicates the formation of the amine adduct $t\mathrm{BuP(NH_2)NH_2{-}AlMe_3}$ (**A**). In addition, a doublet at $\delta = 42.3$ ppm with a typical $^1J_{\mathrm{P,H}}$ coupling constant for a P(V)-H moiety (509 Hz), suggests the formation of either the iminophosphorane adduct $t\mathrm{Bu(H)P(NH_2)NH{-}AlMe_3}$ (**B**) or the methane elimination product $t\mathrm{BuP(NH)_2MMe_2}$ (**C**). At −60 °C, this compound is the only P-containing species present in solution. It disappears on raising the temperature with the subsequent appearance of the final two doublets with similar $^1J_{\mathrm{P,H}}$ coupling constants (490 Hz, 460 Hz) for the *trans* and the *cis* isomer of the eight-membered heterocycle **1**.

In contrast, the ^{31}P NMR spectra obtained from the reaction of $t\mathrm{BuP(NH_2)_2}$ with $\mathrm{GaMe_3}$ and $\mathrm{InMe_3}$ at −60 °C each show a singlet at $\delta = 51.5$ and 49.5 ppm, respectively, indicat-

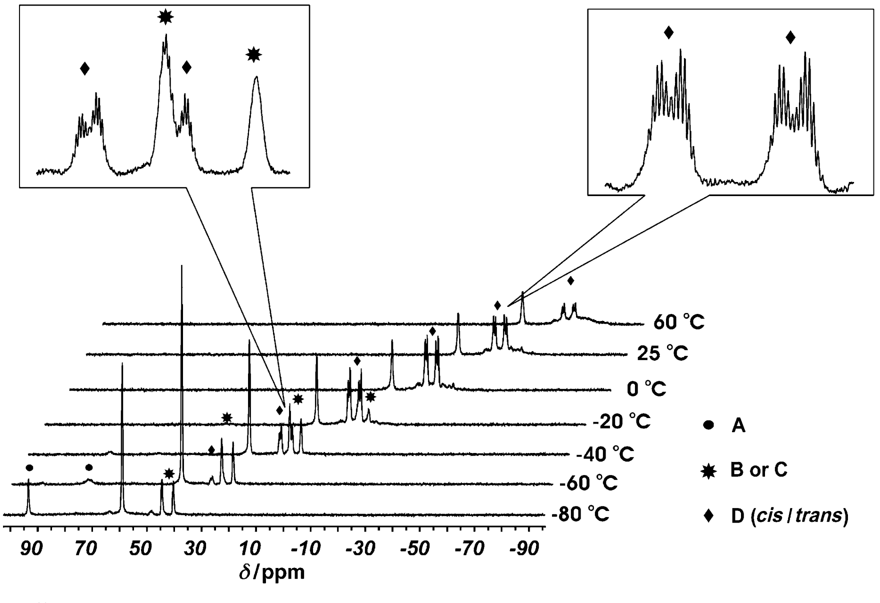

Figure 2. ^{31}P NMR spectra from the reaction of $t\mathrm{BuP(NH_2)_2}$ with $\mathrm{AlMe_3}$ recorded between −60 and +30 °C.

ing the formation of the P-coordinated adducts tBu(H_2N)$_2$P–MMe_3 (**E**). In addition, the spectrum of the $GaMe_3$ reaction also shows a doublet in very low intensity at $\delta = 42.1$ ppm ($^1J_{P,H} = 506$ Hz). Raising the temperature to ambient temperature leads to the formation of the metallophosphinates **2** and **3** (*cis* and *trans* isomers). In sharp contrast to the $AlMe_3$ reaction, the intermediate iminophosphorane adducts of type **B** or the methane elimination products of type **C** are detected in only very small concentrations, demonstrating these species to be only fairly stable in solution.

Quantum-chemical calculations II: To assign the chemical shifts of the reaction intermediates and to establish the reaction pathway with more confidence, we calculated the ^{31}P NMR shifts of all possible reaction intermediates (amine adduct (**A**), phosphine adduct (**E**), iminophosphorane adduct (**B**), intramolecular stabilized four-membered heterocycle (**C**)). The calculated and the experimental values are given in Table 2.

Table 2. BP86/TZVPP-calculated chemical shifts of [tBuP(NH_2)(NH_2MMe_3)], [tBuP(H)(NH_2)($NHMMe_3$)], [tBu(H)P$(NH)_2MMe_2$], and [tBu$(NH_2)_2PMMe_3$] (M = Al, Ga) relative to tBuP$(NH_2)_2$ ($\delta(^{31}P) = 62$ ppm). Available experimental values are given in parentheses.

Compound	M = Al	M = Ga
[tBuP(NH_2)NH_2MMe_3] (**A**)	89 (93)	85 (–)
[tBuP(H)(NH_2)=$NHMMe_3$] (**B**)	34 (–)	33 (–)
[tBuP(MMe_3)$(NH_2)_2$] (**E**)	42 (–)	48 (52)
[tBuP(H)$(NH)_2MMe_2$] (**C**)	40 (42)	43 (42)

The calculated ^{31}P NMR shift of the Me_3Al–amine adduct **A** ($\delta = 89$ ppm) corresponds very well to the experimental value ($\delta = 93$ ppm) for the first reaction intermediate formed at very low temperature. The formation of the phosphine adduct **E** (tBu$(NH_2)_2$P–$AlMe_3$) can clearly be ruled out (calcd: $\delta = 42$ ppm). In contrast, the experimentally obtained ^{31}P NMR shift for the reaction with $GaMe_3$ agrees very well with the calculated value for the corresponding phosphine adduct **E** ($\delta = 48$ ppm (calcd) versus $\delta = 52$ ppm (exptl)). The calculated chemical shift of the amine adduct **A** is significantly shifted to lower field ($\delta = 85$ ppm). These results are in good agreement with Pearson's HSAB principle: the soft Lewis acid $GaMe_3$ prefers coordination to the soft P center, whereas the reaction of the hard $AlMe_3$ Lewis acid occurs at the hard N center. Analogous trends have recently been observed for the reaction of tBuP(NHtBu)$_2$ and MMe_3 (M = Al, Ga, In).[11c] Based on the results of the NMR investigation and the BP86/TZVPP calculations, we propose the reaction scheme given in Scheme 3.

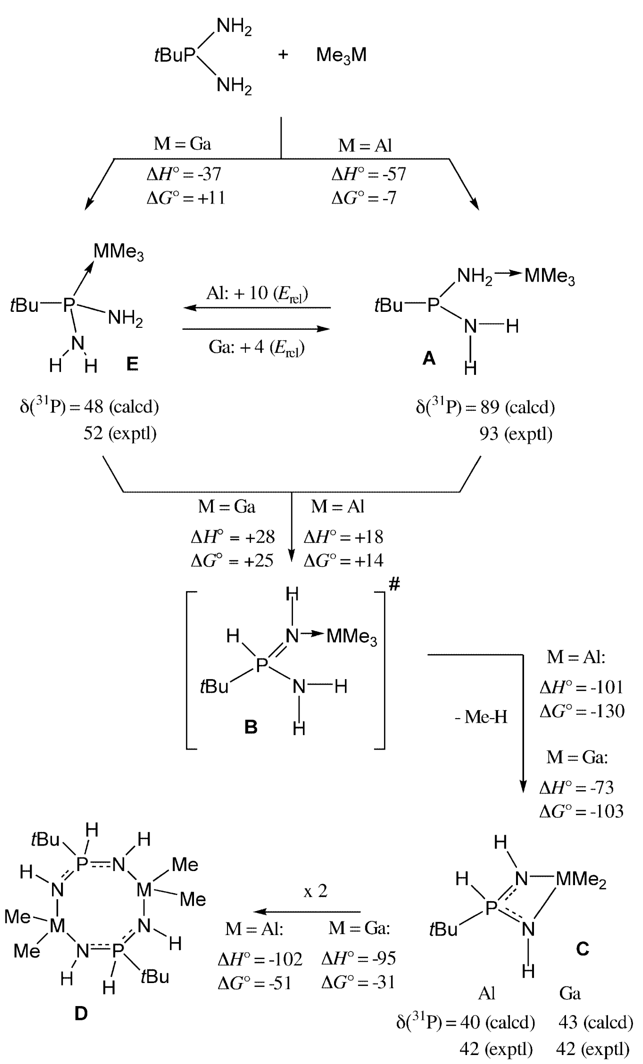

Scheme 3. Most likely formed reaction intermediates of the reaction of tBuP$(NH_2)_2$ with MMe_3 (M = Al, Ga) based on NMR investigations and BP86/TZVPP calculations. $\Delta H°$ and $\Delta G°$ are given in kJ mol^{-1} and include the non-scaled zero point energy and thermal corrections to the enthalpy (Gibbs energy) at 298 K.

Unfortunately, the $AlMe_3$–amine adduct (**A**), which according to DFT calculations is about 10 kJ mol^{-1} more stable than the phosphine adduct **E**, could not be isolated. It shows a strong tendency to react either to the iminophosphorane adduct (type **B**) or, even more likely, to undergo a methane elimination reaction with the consequent formation of the intramolecularly-stabilized four-membered heterocycle tBu(H)P$(NH)_2AlMe_2$ (type **C**), whose formation is strongly supported by the calculated thermodynamics. In sharp contrast, the phosphine adduct formed with $GaMe_3$ (**B**) is stabilized by about 4 kJ mol^{-1} compared to the corresponding amine adduct of type **A**. tBu$(NH_2)_2$P–$GaMe_3$ (**4**) was found to be fairly stable below −30 °C. It was clearly identified by its ^{31}P NMR spectrum, showing a singlet at $\delta = 51.5$ ppm, and its ^{1}H NMR spectrum, which shows resonances due to the tBuP and GaMe moieties in a relative intensity of 1:1. However, due to the tendency of **4** to react in solution with methane elimination, resonances of the heterocycle **2** are also present (about 10 % even at −30 °C). Unfortunately, suitable single crystals of **4** could not be obtained so that the structures of **2** and the other species were calculated by DFT methods (Figure 3).

The calculated bond lengths of the $AlMe_3$ and $GaMe_3$ adducts in Figure 3 are very similar (usually within 1–2 pm). The only exception from this notion are the M–N distances: dative Al–N bonds are significantly shorter than Ga–N

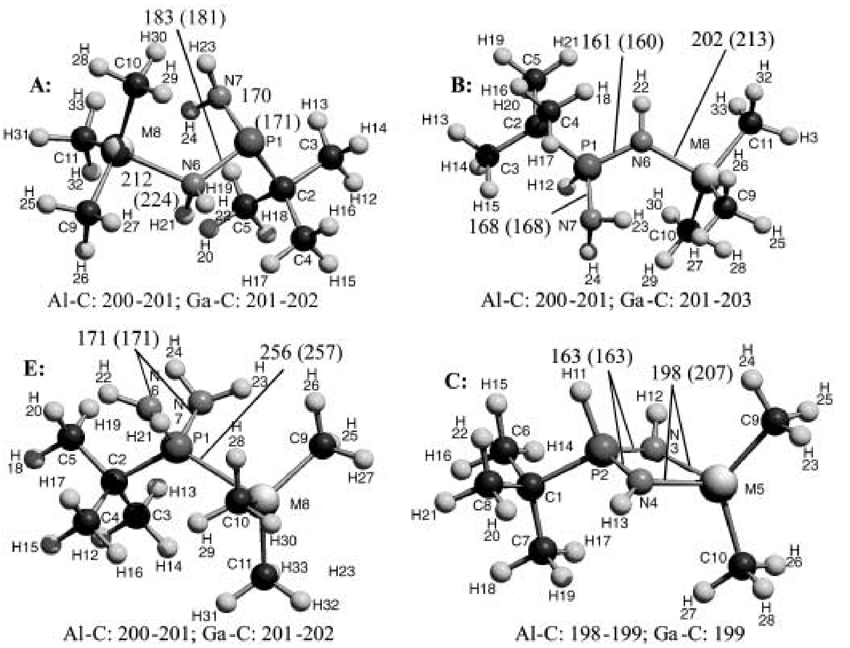

Figure 3. BP86/TZVPP optimized geometries of the proposed reaction intermediates **A**, **B**, **C**, and **E** as well as important bond lengths [pm]. The bond lengths of the Al compounds are given first and those of the Ga compounds in parenthesis. For comparison, the calculated P–N bond lengths in *t*BuP(NH$_2$)$_2$ are 174 pm and those of the P(H) iminophosphorane form *t*Bu(H$_2$N)(H)P=NH are 158 and 170 pm.

bonds (by 11 to 12 pm) as is typical for alane– and gallane–amine adducts. The P–N distance of the coordinated NH$_2$ group in adduct **A** is elongated by 7 to 9 pm upon complexation, whereas the coordinated P=NH moiety of the iminophosphorane adduct **B** is only elongated by 2 to 3 pm compared to free *t*Bu(H$_2$N)P(H)=NH. The methane elimination products **C** show similar P–N and the M–N bond lengths. The short P–N distance of 163 pm reflects the delocalized bonding situation (see also Supporting Information).

Reactions of *t*BuP(NH$_2$)$_2$ with M*t*Bu$_3$ at low temperature: Since no further experimental information on the MMe$_3$ reaction intermediates could be obtained, we extended our studies on reactions of *t*BuP(NH$_2$)$_2$ with sterically more crowded Al*t*Bu$_3$ and Ga*t*Bu$_3$, which were expected to kinetically stabilize the corresponding reaction intermediates.

Reactions of *t*uP(NH$_2$)$_2$ with Al*t*Bu$_3$ and Ga*t*Bu$_3$, respectively, at −30 °C and subsequent storage of the resulting solutions at −60 °C yielded *t*Bu(H$_2$N)(H)P(=NH)–M*t*Bu$_3$ (M = Al **5**, Ga **6**) as colorless solids [Eq. (2)].

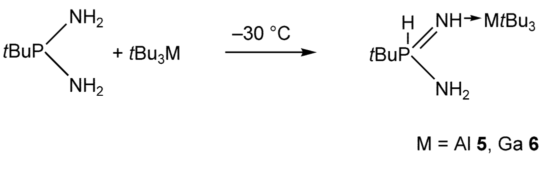

$$t\text{BuP}(\text{NH}_2)_2 + t\text{Bu}_3\text{M} \xrightarrow{-30\,^\circ\text{C}} t\text{BuP}(\text{H})(=\text{NH}\rightarrow \text{M}t\text{Bu}_3)(\text{NH}_2) \quad \text{M = Al } \mathbf{5}, \text{ Ga } \mathbf{6} \tag{2}$$

The ^{31}P NMR spectra of **5** and **6** each show one doublet (**5**: 44.2 ppm (ddz, $^1J_{P,H} = 515$ Hz, $^3J_{P,H} = 18.1$ Hz); **6**: 44.5 ppm (ddz, $^1J_{P,H} = 510$ Hz, $^3J_{P,H} = 17.8$ Hz)) with $^1J_{P,H}$ coupling constants typically observed for P^V centers. ^{1}H NMR spectra show the expected resonances of the *t*BuP, N–H, P–H, and *t*BuM groups, whose integration is consistent with the formation of the iminophosphorane adducts **5** and **6**. The P–H group of **6** shows a hyperfine structure with couplings to the P atom (d, $^1J_{P,H} = 510$ Hz) the imino protons (d, $^3J_{H,H} = 10.6$ Hz) and the amino protons (t, $^3J_{H,H} = 2.2$ Hz), which proof the formation of the iminophosphorane-Ga*t*Bu$_3$ adduct (Figure 4).

In addition, small resonances due to the formation of the corresponding heterocycles are present in the spectra (doublet at $\delta \approx 6.6$ ppm), which demonstrate the lability of both **5** and **6** toward alkane elimination as was already found for the MMe$_3$ derivatives **1**–**3**.

Quantum-chemical calculations III: To obtain further evidence for the formation of the iminophosphorane adducts **5** and **6** we calculated the vibrational frequencies of their fully optimized structures at the BP86/SV(P) level. The simulated and experimental IR spectra of the Al*t*Bu$_3$–iminophosphorane adduct **5** are in very good agreement. In particular the wavenumbers and intensities of the two separate N–H stretches at 3468 cm^{-1} (calcd: 3490 cm^{-1}) and 3377 cm^{-1} (calcd: 3379 cm^{-1}) as well as the P–H stretching vibration at 2366 cm^{-1} (calcd: 2293 cm^{-1}) agree very well (see Supporting Information). The calculated and experimental IR spectra of the Ga*t*Bu$_3$–iminophosphorane adduct **6** are very similar. The very good agreement between experiment and

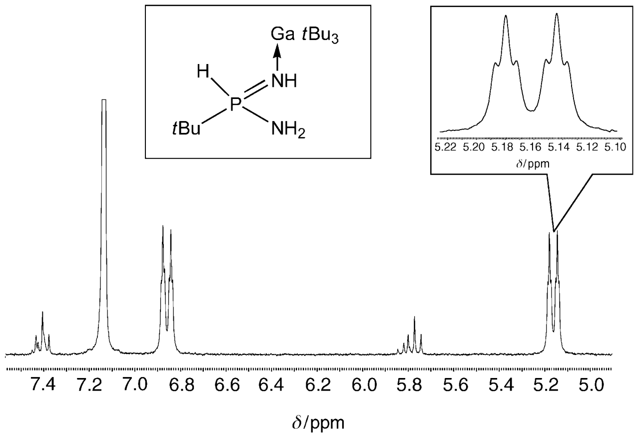

Figure 4. Selected sector of the ^{1}H NMR spectrum of the iminophosphorane–Ga*t*Bu$_3$ adduct **6** showing the hyperfine structure.

theory lends further credibility to the assignment of the isolated compounds as the iminophosphorane adducts **5** and **6**.

The relative stabilities of the aminophosphane adduct **A** versus the iminophosphorane adduct **B** are worthy of comment. From the M*t*Bu$_3$ reactions it was convincingly concluded that the iminophosphorane adduct **B** is formed. However, the DFT calculations suggest that both forms, **A** and **B**, are close in energy in favor of the aminophosphane tautomer **A**. Since **A** and **B** show phosphorus compounds in different oxidation states (+III and +V) and different bonding modes—including only single bonds for **A** but also a P=N double bond for **B**—it appeared likely that for a correct energetic description of both tautomers flexible basis sets and good correlated methods would be needed. Consequently, we optimized the AlR$_3$ adducts **A** and **B** at the BP86 and MP2 levels and increased the size of the basis set from SV(P) to TZVPP. The relative Gibbs energies of these species at 298 K are compared in Table 3.

Table 3. Relative Gibbs energies at 298 K of the two tautomeric forms **A** and **B** of AlR$_3$ adducts (R = Me, *t*Bu) at the BP86 and MP2 levels with SV(P) and TZVPP basis sets [kJ mol^{-1}].

Level	**A** (AlMe$_3$)	**B** (AlMe$_3$)	**A** (Al*t*Bu$_3$)	**B** (Al*t*Bu$_3$)
BP86/SV(P)	0	+25	0	+16
BP86/TZVPP	0	+14	0	+7
MP2/SV(P)	0	+24	–	–
MP2/TZVPP	0	+4	(0)[a]	(−3)[a]

[a] Extrapolated value, see text.

From Table 3 it can be seen that the aminophosphane tautomer **A** is thermodynamically favored (4 to 25 kJ mol^{-1}). However, changing the substituent R of the coordinated trialkylalane AlR$_3$ from Me to *t*Bu, the iminophosphorane adduct **B** is *relatively* stabilized by 7 to 9 kJ mol^{-1}. In addition, increasing the size of the basis set from SV(P) to TZVPP again increases the relative stability of **B** by 9 to 20 kJ mol^{-1}. The use of the best correlated method (MP2) and the largest basis set (TZVPP) for the AlMe$_3$ adduct **B** reduces the energetic difference between the tautomers **B** and **A** to 4 kJ mol^{-1}. Unfortunately, due to the size of the system we could not optimize the structures of the two tautomeric Al*t*Bu$_3$ adducts at the MP2/TZVPP level.[18] Considering the Al*t*Bu$_3$–iminophosphorane adduct **B** at the BP86/TZVPP level to be stabilized by 7 kJ mol^{-1} compared to the AlMe$_3$ adduct **B**, it is reasonable to conclude that at the higher MP2/TZVPP level a similar stabilization of the Al*t*Bu$_3$–iminophosphorane adduct **B** should be expected. Therefore, the missing component of the relative Gibbs energy of the Al*t*Bu$_3$–iminophosphorane adduct **B** with MP2/TZVPP is estimated to be about −3 kJ mol^{-1} (+4 kJ mol^{-1} minus 7 kJ mol^{-1}), thus favoring the formation of the iminophosphorane–Al*t*Bu$_3$ adduct of type **B**. This is in agreement with the experimental findings.

From the calculations it may be stated that the correct energetic description of the P$^{\mathrm{III}}$ and P$^{\mathrm{V}}$ adducts **A** and **B** is very delicate. Taking into consideration the size of the system, it is impossible for us to use higher correlated methods than MP2 (i.e. MP4 or CCSD(T)) and larger basis sets than TZVPP (i.e. cc-pVQZ).[18] From the analysis of Table 3 it seems reasonable to conclude that at such a high level (i.e. CCSD(T)/cc-pVQZ) the iminophosphorane structure **B** represents the global minimum, however, a direct proof for this conclusion awaits highly correlated computational methods applicable on systems of the given size.

M*t*Bu$_3$ reactions at ambient temperature: Reaction of *t*BuP(NH$_2$)$_2$ with *t*Bu$_3$Al and *t*Bu$_3$Ga, respectively, at ambient temperature led to the formation of [{*t*Bu(H)P(NH)$_2$M(*t*Bu)$_2$}$_2$] (M = Al **7**, Ga **8**; [Eq. (3)]) as is demonstrated by ^{1}H and ^{31}P NMR spectroscopy.

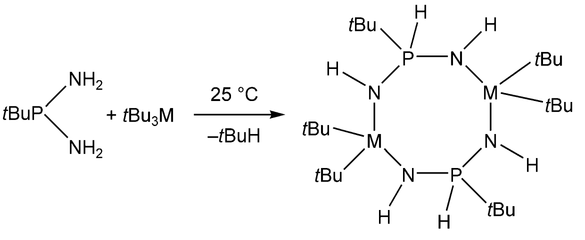

M = Al **7**, Ga **8**

(3)

Again, two sets of doublets with $^1J_{\mathrm{P,H}}$ coupling constants between 470 and 515 Hz are observed in the ^{31}P NMR spectra of **7** and **8** according to the typical formation of both the *cis* and *trans* isomers. Consequently, ^{1}H NMR spectra also show two sets of resonances due to the organic groups. The presence of both N–H and P–H groups is confirmed by IR spectroscopy. The spectra of **7** and **8** show strong N–H adsorption bands at 3170 cm^{-1} (**7**) and 3375 and 3360 cm^{-1} (**8**) as well as P–H absorption bands at 2363 cm^{-1} (**7**) and 2355 cm^{-1} (**8**).

Conclusion

According to variable-temperature (VT) NMR investigations, *t*BuP(NH$_2$)$_2$ reacts with Group 13 trialkyl compounds MR$_3$ (M = Al, Ga, In; R = Me, *t*Bu) with the initial formation of aminophosphane adducts, which undergo 1,2-H shift with the subsequent formation of iminophosphorane adducts. Finally, alkane elimination reactions yield metallonitridophosphinates. Alanes AlR$_3$ initially form amine adducts, whereas the less Lewis acidic gallanes and indanes prefer coordination by the softer phosphorus atom. The stability of the subsequently formed iminophosphorane adducts depends on the steric demand of the Lewis acid. *t*Bu$_3$M (M = Al, Ga) adducts were found to be fairly stable at low temperature, whereas the corresponding MMe$_3$ adducts could not be isolated. BP86/TZVPP (DFT) calculations verified the proposed reaction pathway and gave insights into the thermodynamics of the reaction. The central Group 13 element was found to have a significant influence on the stability of both the reaction intermediates and the finally formed heterocycles.

Experimental Section

General considerations: All manipulations were performed in a glove box under an argon atmosphere or by standard Schlenk techniques. Solvents were distilled from sodium benzophenone ketyl or Na/K alloy prior to use. *t*BuP(NH$_2$)$_2$,[6] GaMe$_3$,[19] InMe$_3$,[20] Al*t*Bu$_3$[21] and Ga(*t*Bu)$_3$[22] were prepared according to literature methods, whereas AlMe$_3$ was commercially available (Aldrich) and used as received. NMR spectra were recorded using a Bruker DPX 300 spectrometer. ^{1}H and ^{13}C{^{1}H} spectra are referenced to the resonances of the solvents C_6D_6 ($\delta(^{1}H)=7.15$ ppm, $\delta(^{13}C)=128.0$ ppm) and [D$_8$]toluene ($\delta(^{1}H)=7.09$ ppm, $\delta(^{13}C)=137.5$ ppm); ^{31}P{^{1}H} spectra are referenced to external H_3PO_4 ($\delta(^{31}P)=0$ ppm). Infrared spectra were recorded between KBr plates using a Bruker Vector 22 spectrometer. Mass spectra were recorded on a VG Masslab 12–250 spectrometer in the electron impact mode (EI). Melting points were measured in wax-sealed capillaries and are not corrected. Elemental analyses were performed at the Mikroanalytisches Labor der Universität Bonn.

General preparation for [{*t*Bu(H)P(NH)$_2$MMe$_2$}$_2$]: At −78 °C a solution of MMe$_3$ (2 mmol) in hexane (30 mL) was slowly added to *t*BuP(NH$_2$)$_2$ (0.24 g, 2 mmol) dissolved in hexane (30 mL). The resulting solution was slowly warmed to ambient temperature, leading to a smooth gas evolution, stirred for an additional 2 h and concentrated to 10 mL. Storage at −30 °C for 24 h gave colorless crystals.

[{*t*Bu(H)P(NH)$_2$AlMe$_2$}$_2$] (1): M.p. 125 °C; yield 0.23 g (65 %); elemental analysis calcd (%) for $C_{12}H_{36}Al_2N_4P_2$ ($M_r=352.35$): C: 40.90, H 10.30; found: C 40.45, H 10.15; ^{31}P, ^{1}H, and ^{13}C NMR spectra in C_6D_6 at ambient temperature show a mixture of the *cis* and *trans* isomer (35:65). ^{1}H NMR (300 MHz, C_6D_6, 30 °C): $\delta=-0.43$ (s, 6 H; AlCH$_3$, *cis*), −0.40 (s, 12 H; AlCH$_3$, *trans*), −0.37 (s, 6 H; AlCH$_3$, *cis*), 0.63 (d, $^{3}J_{P,H}=17.0$ Hz, 36 H; PC(CH$_3$)$_3$, *cis*/*trans*), 0.93 (s (br), 8 H; NH, *cis*/trans), 6.25 (dt, $^{1}J_{P,H}=492$ Hz, $^{3}J_{P,H}=7.4$ Hz, 2 H; PH, *trans*), 6.27 ppm (dt, $^{1}J_{P,H}=481$ Hz, $^{3}J_{P,H}=5.9$ Hz, 2 H; PH, *cis*); ^{13}C NMR (75 MHz, C_6D_6, 30 °C): $\delta=22.9$ (d, $^{2}J_{P,C}=2.9$ Hz; PC*Me*$_3$, *cis*), 23.3 (d, $^{2}J_{P,C}=2.9$ Hz; PC*Me*$_3$, *trans*), 30.6 (d, $^{1}J_{P,C}=74.7$ Hz; P*C*Me$_3$, *trans*), 30.8 (d, $^{1}J_{P,C}=74.7$ Hz; P*C*Me$_3$, *cis*); ^{31}P NMR (120 MHz, C_6D_6, 30 °C): $\delta=46.0$ (ddz, $^{1}J_{P,H}=492$ Hz, $^{3}J_{P,H}=17.0$ Hz; *trans*), 46,7 ppm (ddz, $^{1}J_{P,H}=464$ Hz, $^{3}J_{P,H}=17.6$ Hz; *cis*); IR (Nujol): $\tilde{\nu}=3377$, 3338, 3318 (N−H), 2364, 2325 (P−H), 1188, 1165, 967, 944, 925, 700, 669 cm^{-1}; EI-MS (16 eV, 150 °C): *m*/*z* (%): 353 (1) [*M*]$^+$, 339 (68) [*M*−Me]$^+$, 322 (100) [*M*−2 Me]$^+$, 265 (22) [*M*−2 Me−*t*Bu]$^+$, 161 (2) [*t*BuP(NH)N(H)Al(H)Me]$^+$.

[{*t*Bu(H)P(NH)$_2$GaMe$_2$}$_2$] (2): M.p. 130 °C; yield 0.24 g (55 %); elemental analysis calcd (%) for $C_{12}H_{36}Ga_2N_4P_2$ ($M_r=437.83$): C 32.92, H 8.29; found: C 32.26, H 8.12; ^{31}P, ^{1}H, and ^{13}C NMR spectra in C_6D_6 at ambient temperature show a mixture of the *cis* and *trans* isomer (40:60). ^{1}H NMR (300 MHz, C_6D_6, 30 °C): $\delta=-0.11$ (s, 6 H; GaCH$_3$, *cis*), −0.07 (s, 12 H; GaCH$_3$, *trans*), −0.02 (s, 6 H; GaCH$_3$, *cis*), 0.71 (d, $^{3}J_{P,H}=16.7$ Hz, 18 H; PC(CH$_3$)$_3$, *cis*), 0.72 (d, $^{3}J_{P,H}=16.6$ Hz, 18 H; PC(CH$_3$)$_3$, *trans*), 0.78 (s (br), 8 H; NH, *cis*/*trans*), 6.27 (dt, $^{1}J_{P,H}=487$ Hz, $^{3}J_{P,H}=8.2$ Hz, 2 H; PH, *trans*), 6.37 ppm (dt, $^{1}J_{P,H}=475$ Hz, $^{3}J_{P,H}=5.8$ Hz, 2 H; PH, *cis*); ^{13}C NMR (75 MHz, C_6D_6, 30 °C): $\delta=-6.5$ (s (br); GaMe$_3$, *cis*/*trans*), 23.3 (d, $^{2}J_{P,C}=2.9$ Hz; PC*Me*$_3$, *cis*), 23.8 (d, $^{2}J_{P,C}=2.9$ Hz; PC*Me*$_3$, *trans*), 31.1 (d, $^{1}J_{P,C}=74.4$ Hz; P*C*Me$_3$, *trans*), 31.3 (d, $^{1}J_{P,C}=74.4$ Hz; P*C*Me$_3$, *cis*); ^{31}P NMR (120 MHz, C_6D_6, 30 °C): $\delta=46.5$ (ddz, $^{1}J_{P,H}=487$ Hz, $^{3}J_{P,H}=16.5$ Hz; *trans*), 47.3 (ddz, $^{1}J_{P,H}=475$ Hz, $^{3}J_{P,H}=16.8$ Hz, *cis*); IR (Nujol): $\tilde{\nu}=3390$, 3363 (N−H), 2357, 2312 (P−H), 1191, 1129, 986, 926, 816, 724, 668 cm^{-1}; EI-MS (12 eV, 175 °C): *m*/*z* (%): 423 (90) [*M*$^+$−Me], 406 (40) [*M*−2 Me−H]$^+$, 320 (20) [*M*−2 Me−P*t*Bu]$^+$, 303 (80) [*M*−3 Me−P*t*Bu]$^+$, 219 (10) [*M*/2]$^+$, 203 (100) [*M*/2−MeH]$^+$.

[{*t*Bu(H)P(NH)$_2$InMe$_2$}$_2$] (3): M.p. 112 °C; yield 0.29 g (55 %); elemental analysis calcd (%) for $C_{12}H_{36}In_2N_4P_2$ ($M_r=528.02$): C 27.30, H 6.87; found: C 26.82, H 6.75; ^{1}H NMR (300 MHz, C_6D_6, 30 °C): $\delta=0.01$ (s, 12 H; InCH$_3$), 0.61 (s (br), 4 H; NH), 0.73 (d, $^{3}J_{P,H}=16.4$ Hz, 18 H; PC(CH$_3$)$_3$), 6.39 ppm (d (br), $^{1}J_{P,H}=469$ Hz, 2 H; PH); ^{13}C NMR (75 MHz, C_6D_6, 30 °C): $\delta=23.5$ (m (br); PC*Me*$_3$), 31.8 ppm (d, $^{1}J_{P,C}=71.8$ Hz; P*C*Me$_3$); ^{31}P NMR (120 MHz, C_6D_6, 30 °C): $\delta=51.4$ ppm (d (br), $^{1}J_{P,H}=469$ Hz); IR (Nujol): $\tilde{\nu}=3383$, 3359 (N−H), 2285 (P−H), 1260, 1087, 1048, 975, 939, 811, 695 cm^{-1}; EI-MS (12 eV, 75 °C): *m*/*z* (%): 513 (18) [*M*−Me]$^+$, 248 (11) [*t*BuP(H)N(H)InMe$_2$]$^+$, 192 (21) [P(H)N(H)InMe$_2$]$^+$, 144 (100) [In(Me)$_2$]$^+$.

[*t*BuP(NH$_2$)$_2$−GaMe$_3$] (4): A solution of *t*BuP(NH$_2$)$_2$ (0.24 g, 2 mmol) in hexane (20 mL) was combined at −78 °C with a solution of GaMe$_3$ (0.23 g, 2 mmol) in hexane (10 mL). The resulting solution was slowly warmed to −30 °C (no gas evolution!) and stored for 24 h at −60 °C, resulting in the formation of a colorless crystalline solid.

M.p. 36 °C (decomp); yield 0.23 g (50 %); elemental analysis calcd (%) for $C_7H_{22}GaN_2P$ ($M_r=234.96$): C: 35.78, H 9.44; found: C 35.31, H 9.09; ^{1}H NMR (300 MHz, C_6D_6, 30 °C): $\delta=-0.01$ (s, 9 H; Ga(CH$_3$)$_3$), 0.76 (d, $^{3}J_{P,H}=14.5$ Hz, 9 H; PC(CH$_3$)$_3$), 1.35 ppm (s (br), 4 H; NH); ^{13}C NMR (75 MHz, C_6D_6, 30 °C): $\delta=-6.0$ (s (br); GaMe$_3$), 24.3 (d, $^{2}J_{P,C}=8.4$ Hz; PCMe$_3$), 32.1 ppm (d, $^{1}J_{P,C}=27.8$ Hz; PCMe$_3$); ^{31}P NMR (120 MHz, C_6D_6, 30 °C): $\delta=56.4$ ppm (s); EI-MS (12 eV, 100 °C): *m*/*z* (%): 219 (77) [*M*−Me]$^+$, 203 (22) [*M*−2 Me]$^+$, 120 (17) [*M*−GaMe$_3$]$^+$, 99 (100) [GaMe$_2$]$^+$, 63 (94) [*M*−GaMe$_3$−*t*Bu]$^+$.

General preparation of [*t*Bu(H)P(NH)NH$_2$−M*t*Bu$_3$]: M*t*Bu$_3$ (2 mmol) and *t*BuP(NH$_2$)$_2$ (0.24 g, 2 mmol) dissolved in hexane (20 mL) were combined at −78 °C. The resulting solution was slowly warmed to −30 °C, stirred for 15 min, and then stored for 24 h at −60 °C. Colorless crystalline solids were formed.

[*t*Bu(H)P(NH)NH$_2$−Al*t*Bu$_3$] (5): M.p. 85 °C (decomp); yield 0.51 g (80 %); elemental analysis calcd (%) for $C_{16}H_{40}AlN_2P$ ($M_r=318.46$): C 60.34, H 12.66; found: C 59.92, H 12.37; ^{1}H NMR (300 MHz, C_6D_6, 30 °C): $\delta=0.43$ (d, $^{3}J_{P,H}=17.9$ Hz, 9 H; PC(CH$_3$)$_3$), 1.21 (m (br), 2 H; NH$_2$), 1.33 (s (br), 1 H; NH), 1.37 (s, 27 H; AlC(CH$_3$)$_3$), 6.01 ppm (dd, $^{1}J_{P,H}=515$ Hz, $^{3}J_{H,H}=10.4$ Hz, 1 H; PH); ^{13}C NMR (75 MHz, C_6D_6, 30 °C): $\delta=22.7$ (d, $^{2}J_{P,C}=2.3$ Hz; P*C*Me$_3$), 23.4 (s; Al(*C*Me$_3$)$_3$), 31.2 (d, $^{1}J_{P,C}=184$ Hz; PC*Me*$_3$), 33.4 ppm (s; Al(C*Me*$_3$)$_3$); ^{31}P NMR (120 MHz, C_6D_6, 30 °C): $\delta=44.2$ ppm (ddz, $^{1}J_{P,H}=515$ Hz, $^{3}J_{P,H}=18.1$ Hz); IR (Nujol): $\tilde{\nu}=3472$, 3381, 3350 (N−H), 2392 (P−H), 1543, 996, 928, 612 cm^{-1}; EI-MS (12 eV, 50 °C): *m*/*z* (%): 57 (10) *t*Bu$^+$, 63 (100) [*M*−Al*t*Bu$_3$−*t*Bu]$^+$, 120 (60) [*M*−Al*t*Bu$_3$]$^+$, 203 (4) [*M*−2 *t*Bu−H]$^+$, 261 (3) [*M*−*t*Bu]$^+$.

[*t*Bu(H)P(NH)NH$_2$−Ga*t*Bu$_3$] (6): M.p. 65 °C (decomp); yield 0.61 g (85 %); elemental analysis calcd (%) for $C_{16}H_{40}GaN_2P$ ($M_r=361.20$): C 53.20, H 11.16; found: C 52.71, H 10.79; ^{1}H NMR (300 MHz, C_6D_6, 30 °C): $\delta=0.48$ (d, $^{3}J_{P,H}=17.6$ Hz, 9 H; PC(CH$_3$)$_3$), 1.27 (m (br), 2 H; NH$_2$), 1.56 (s (br), 1 H; NH), 1.42 (s, 27 H; GaC(CH$_3$)$_3$), 6.03 ppm (ddt, $^{1}J_{P,H}=510$ Hz, $^{3}J_{H,H}=10.6$ Hz, $^{3}J_{H,H}=2.2$ Hz, 1 H; PH); ^{13}C NMR (75 MHz, C_6D_6, 30 °C): $\delta=22.9$ (d, $^{2}J_{P,C}=2.6$ Hz; P*C*Me$_3$), 33.2 (s (br); PC*Me*$_3$), 33.6 ppm (s; Ga(C*Me*$_3$)$_3$); ^{31}P NMR (120 MHz, C_6D_6, 30 °C): $\delta=44.5$ ppm (ddz, $^{1}J_{P,H}=510$ Hz, $^{3}J_{P,H}=17.8$ Hz); IR (Nujol): $\tilde{\nu}=3473$, 3379, 3362 (N−H), 2356 (P−H), 1538, 1403, 1349, 1158, 932, 612 cm^{-1}.

General preparation of[{*t*Bu(H)P(NH)$_2$M*t*Bu$_2$}$_2$]: M*t*Bu$_3$ (2 mmol) and *t*BuP(NH$_2$)$_2$ (0.24 g, 2 mmol) dissolved in hexane (20 mL) were combined at −78 °C. The resulting solution was slowly warmed to ambient temperature and stirred for 2 h. Colorless solids were formed, which were filtered and recrystallized from a solution in toluene at −60 °C.

[{*t*Bu(H)P(NH)$_2$Al*t*Bu$_2$}$_2$] (7): M.p. 210 °C; yield 0.23 g (45 %); elemental analysis calcd (%) for $C_{24}H_{60}Al_2N_4P_2$ ($M_r=520.67$): C 55.36, H 11.62; found: C 55.02, H 11.39; ^{31}P, ^{1}H, and ^{13}C NMR spectra in C_6D_6 at ambient temperature show a mixture of the *cis* and *trans* isomer (50:50). ^{1}H NMR (300 MHz, C_6D_6, 30 °C): $\delta=0.73$ (d, $^{3}J_{P,H}=17.1$ Hz, 36 H; PC*(CH$_3$)$_3$*, *cis*/*trans*), 0.97 (m (br), 8 H; NH, *cis*/*trans*), 1.22 (s (br), 54 H; AlC(CH$_3$)$_3$, *trans*), 1.23 (s, 18 H; AlC(CH$_3$)$_3$, *cis*), 6.57 (dt, $^{1}J_{P,H}=497$ Hz, $^{3}J_{H,H}=8.7$ Hz, 2 H; PH, *trans*), 6.58 ppm (dt, $^{1}J_{P,H}=487$ Hz, $^{3}J_{H,H}=7.5$ Hz, 2 H; PH, *cis*); ^{13}C NMR (75 MHz, C_6D_6, 30 °C): $\delta=23.6$ (d, $^{2}J_{P,C}=2.6$ Hz; PC*Me*$_3$, *cis*), 23.7 (d, $^{2}J_{P,C}=2.3$ Hz; PC*Me*$_3$, *trans*), 31.5 (s; AlC*Me*$_3$, *cis*), 31.6 (s; AlC*Me*$_3$, *cis*), 31.8 ppm (s; AlC*Me*$_3$, *trans*); ^{31}P NMR (120 MHz, C_6D_6, 30 °C): $\delta=47.3$ (ddz, $^{1}J_{P,H}=515$ Hz, $^{3}J_{P,H}=17.2$ Hz, *trans*), 48.0 ppm (ddz, $^{1}J_{P,H}=487$ Hz, $^{3}J_{P,H}=17.2$ Hz, *cis*); IR (Nujol): $\tilde{\nu}=3170$ (N−H), 2363 (P−H), 1145, 950, 719, 667 cm^{-1}; EI-MS (12 eV, 100 °C): *m*/*z* (%): 463 (100) [*M*−*t*Bu−H]$^+$, 405 (49) [*M*−2*t*Bu−H]$^+$, 277 (39) [*M*−4*t*Bu−NH−H]$^+$, 57 (39) *t*Bu$^+$.

[{*t*Bu(H)P(NH)$_2$Ga*t*Bu$_2$}$_2$] (8): M.p. 232 °C (decomp); yield 0.36 g (60 %); elemental analysis calcd (%) for $C_{24}H_{60}Ga_2N_4P_2$ ($M_r=606.15$): C 47.56, H 9.98; C 46.98, H 9.67; ^{1}H and ^{13}C NMR spectra in C_6D_6 at ambient temperature show a mixture of the *cis* and *trans* isomer (25:75). ^{1}H NMR (300 MHz, C_6D_6, 30 °C): $\delta=0.81$ (d, $^{3}J_{P,H}=16.4$ Hz, 18 H; PC(CH$_3$)$_3$, *trans*), 0.82 (d, $^{3}J_{P,H}=16.4$ Hz, 18 H; PC(CH$_3$)$_3$, *cis*), 1.27 (s, 36 H; GaC(CH$_3$)$_3$, *trans*), 1.29 (s, 18 H; GaC(CH$_3$)$_3$, *cis*), 1.42 (m (br), 8 H; NH, *cis*/*trans*), 6.61 (dt, $^{1}J_{P,H}=490$ Hz, $^{3}J_{H,H}=8.5$ Hz, 2 H; PH, *trans*), 6.64 ppm (dt, $^1J_{P,H}=482$ Hz, $^3J_{H,H}=7.8$ Hz, 2 H; PH, *cis*); ^{13}C NMR (75 MHz, C_6D_6, 30 °C): $\delta=24.1$ (d, $^2J_{P,C}=2.6$ Hz; PCMe$_3$, *cis*), 24.1 (d, $^2J_{P,C}=2.6$ Hz; PCMe$_3$, *trans*), 31.4 (s; GaC*Me*$_3$, *cis*), 31.6 (s; GaC*Me*$_3$, *trans*), 31.8 ppm (s; GaC*Me*$_3$, *cis*); ^{31}P NMR (120 MHz, C_6D_6, 30 °C): $\delta=49.7$ (ddz, $^1J_{P,H}=490$ Hz, $^3J_{P,H}=16.3$ Hz, *trans*), 50.7 ppm (ddz, $^1J_{P,H}=465$ Hz, $^3J_{P,H}=16.5$ Hz, *cis*); IR (Nujol): $\tilde{\nu}=3375$, 3360, 3349 (N–H), 2355 (P–H), 1161, 983, 948, 937, 614 cm^{-1}; EI-MS (20 eV, 150 °C): *m*/*z* (%): 549 (100) $[M-t\mathrm{Bu}]^+$, 245 (87) $[M-6t\mathrm{Bu}-\mathrm{NH}-4\,\mathrm{H}]^+$, 491 (3) $[M-2t\mathrm{Bu}-\mathrm{H}]^+$, 63 (3) $[\mathrm{P(NH_2)_2}]^+$.

X-ray structure solution and refinement. Crystallographic data of **1** are summarized in Table 4, Figure 1 shows the ORTEP diagram (50 % probability ellipsoids) of its solid-state structure. Data were collected on a Nonius KappaCCD diffractometer. The structure was solved by Patterson methods (SHELXS-97)[23] and refined by full-matrix least-squares on F^2. All non-hydrogen atoms were refined anisotropically and hydrogen atoms were refined by a riding model (SHELXL-97).[24] CCDC-217870 contains the supplementary crystallographic data for this paper. These data can be obtained free of charge via www.ccdc.can.ac.uk/conts/retrieving.html (or from the Cambridge Crystallographic Centre, 12 Union Road, Cambridge CB21EZ, UK; Fax: (+44)1223-336033; or deposit@ccdc.cam.ac.uk).

Table 4. Crystal data and structure refinement of **1**.

formula	$C_{12}H_{16}Al_2N_4P_2$
M_r	352.35
T [K]	123(2)
λ [Å]	0.71073 (Mo$_{K\alpha}$)
crystal system	monoclinic
space group	$P2_1/n$ (no. 14)
unit cell dimensions	
a [Å]	10.0212(2)
b [Å]	6.5113(1)
c [Å]	16.4093(4)
β [°]	98.785(1)
V [Å^3]	1058.16(4)
Z, ρ_{calcd} [g cm^{-3}]	2, 1.106
µ [mm^{-1}]	0.287
crystal size [mm^3]	0.25 × 0.20 × 0.15
θ range for data collection [°]	2.99–24.99
reflections collected/unique	11725/1854 ($R_{int}=0.0355$)
refined parameters	100
goodness-of-fit on F^2	1.067
final $R1$ indices [$I>2\sigma$(I)]	0.0336
$wR2$ indices (all data)	0.0957
residual electron density [e Å^{-3}]	0.603/−0.219

Computational details: All computations were done with the program TURBOMOLE.[25] The geometries of all species were optimized at the (RI-)BP86 level[26] with the split valence polarization SV(P)[27] as well as the triple zeta TZVPP[28] basis set (2d, 1f polarization functions). The nature of the stationary points as true minima was verified by a frequency calculation (no imaginary Eigenvalues) using the new version of AOFORCE[29] at the (RI-)BP86/SV(P) level. Thermal contributions to the enthalpy and the Gibbs energy at 298 K were obtained by standard statistical thermodynamics calculations included in TURBOMOLE with the program FreeH that are based on the calculated (RI-)BP86/SV(P) geometry and IR frequencies. NMR shielding tensors were obtained at the BP86/TZVPP level using the program MPSHIFT included with TURBOMOLE. The calculated chemical shifts were referenced with respect to the experimental position of $t\mathrm{BuP(NH_2)_2}$ of $\delta(^{31}\mathrm{P})=62$ ppm. Additional full optimizations were done at the (RI-)MP2 ab initio level[30,31] with SV(P) and TZVPP basis sets. The IR spectrum of compound **5** was simulated by a superposition of Gauss functions of the calculated IR spectrum at the (RI-)BP86/SV(P) level. Graphic representations, *x*,*y*,*z* coordinates, total energies, and zero-point vibrational energies (ZPVEs) of important computed species are given in the Supporting Information, others may be obtained from the authors (I.K.) upon request. The total energies, ZPEs, number of imaginary frequencies *n*(imag), thermal contributions to the enthalpy ($H°$), and the Gibbs energy ($G°$) at 298 K of all species included in Scheme 3 are also given in the Supporting Information.

Acknowledgment

S. Schulz gratefully acknowledges financial support by the DFG, the Fonds der Chemischen Industrie, the Bundesministerium für Bildung und Forschung (BMBF), and Prof. E. Niecke, Universität Bonn. I. Krossing thanks the DFG and the Fonds der Chemischen Industrie for financial support.

---

[1] Initial reports go back to early studies of Michaelis: a) A. Michaelis, H. von Soden, *Ann. Chem.* **1885**, *229*, 334; b) A. Michaelis, G. Schulze, *Chem. Ber.* **1893**, *26*, 2937; c) A. Michaelis, G. Schulze, *Chem. Ber.* **1894**, *27*, 2572; d) A. Michaelis, K. Luxembourg, *Chem. Ber.* **1895**, *28*, 2205.

[2] a) A. Tarassoli, R. C. Haltiwanger, A. D. Norman, *Inorg. Nucl. Chem. Lett.* **1980**, *16*, 27; b) A. Tarassoli, R. C. Haltiwanger, A. D. Norman, *Inorg. Chem.* **1982**, *21*, 2684.

[3] a) P. B. Hitchcock, H. A. Jasim, M. F. Lappert, H. D. Williams, *J. Chem. Soc. Chem. Commun.* **1986**, 1634; b) J.-T. Ahlemann, H. W. Roesky, R. Murugavel, E. Parisini, M. Noltemeyer, H.-G. Schmidt, O. Müller, R. Herbst-Irmer, L. N. Markovskii, Y. G. Shermolovich, *Chem. Ber.* **1997**, *130*, 1113.

[4] See for instance: a) S. M. Aucott, A. M. Z. Slawin, J. D. Woollins, *J. Chem. Soc. Dalton Trans.* **2000**, 2559; b) T. G. Wetzel, S. Dehnen, P. W. Roesky, *Angew. Chem.* **1999**, *111*, 1155; *Angew. Chem. Int. Ed.* **1999**, *38*, 1086; c) V. V. Kotov, E. V. Avtomonov, J. Sundermeyer, K. Harms, D. A. Lemenovskii, *Eur. J. Inorg. Chem.* **2002**, 678; d) N. Poetschke, M. Nieger, M. A. Khan, E. Niecke, M. T. Ashby, *Inorg. Chem.* **1997**, *36*, 4087; e) O. Kuhl, S. Blaurock, J. Sieler, E. Hey-Hawkins, *Polyhedron* **2001**, *20*, 111; f) U. Florke, H.-J. Haupt, *Z. Kristallogr.* **1993**, *205*, 127.

[5] O. J. Scherer, P. Klusmann, *Angew. Chem.* **1968**, *80*, 541; *Angew. Chem. Int. Ed. Engl.* **1968**, *7*, 560.

[6] a) O. J. Scherer, P. Klusmann, *Z. Anorg. Allg. Chem.* **1969**, *370*, 171; b) G. Schick, A. Loew, M. Nieger, K. Airola, E. Niecke, *Chem. Ber.* **1996**, *129*, 911.

[7] a) A. Kodama, R. W. Parry, *J. Inorg. Nucl. Chem.* **1961**, *17*, 125; b) C. E. Nordman, *Acta. Cryst.* **1960**, *13*, 535.

[8] a) H. Nöth, H. Reith, V. Thorn, *J. Organomet. Chem.* **1978**, *159*, 165; b) A. Gieren, F. C. Ruiz-Pérez, T. Hübner, M. Herberhold, K. Schamel, K. Guldner, *J. Organomet. Chem.* **1989**, *366*, 105; c) B. Wrackmeyer, K. Schamel, M. Herberhold, *Z. Naturforsch. B* **1989**, *44*, 55.

[9] Its synthesis was claimed by Becke-Göhring in 1958, but the resulting product could not be isolated and characterized in its pure form.

[10] S. Schulz, M. Raab, M. Nieger, E. Niecke, *Organometallics* **2000**, *19*, 2616.

[11] a) S. Schulz, T. Bauer, M. Nieger, *Chem. Commun.* **1999**, 879; b) T. Bauer, S. Schulz, M. Nieger, *Z. Anorg. Allg. Chem.* **2001**, *627*, 266; c) T. Bauer, S. Schulz, M. Nieger, U. Kessler *Organometallics* **2003**, *22*, 3134.

[12] A. Schmidpeter, H. Roßknecht, *Angew. Chem.* **1969**, *81*, 572; *Angew. Chem. Int. Ed. Engl.* **1969**, *8*, 614.

[13] See the following and references therein: M. Raab, A. Sundermann, G. Schick, A. Loew, M. Nieger, W. W. Schoeller, E. Niecke, *Organometallics* **2001**, *20*, 1770.

[14] S. Schulz, T. Bauer, M. Nieger, I. Krossing, *Chem. Commun.* **2002**, 1422.

[15] For references see: a) J. Pinkas, D. Chakraborty, Y. Yang, R. Murugavel, M. Noltemeyer, H. W. Roesky, *Organometallics* **1999**, *18*, 523; b) M. R. Mason, M. S. Mashuta, J. F. Richardson, *Angew. Chem.* **1997**, *109*, 247; *Angew. Chem. Int. Ed. Engl.* **1997**, *36*, 239; c) J. M. Corker, D. J. Browning, M. Webster, *Acta Crystallogr.* **1996**, *52*, 583; d) F. E. Hahn, B. Schneider, F.-W. Reier, *Z. Naturforsch. B* **1990**, *45*, 134; e) D. J. Browning, J. M. Corker, M. Webster, *Acta Crystallogr.* **1996**, *52*, 882; f) T. Azais, L. Bonhomme-Coury, J. Vaissermann, P.

Bertani, J. Hirschinger, J. Maquet, C. Bonhomme, *Inorg. Chem.* **2002**, *41*, 981.

[16] For recent reviews see: a) J. K. Brask, T. Chivers, *Angew. Chem.* **2001**, *113*, 4082; *Angew. Chem. Int. Ed.* **2001**, *40*. 3960; b) A. Steiner, S. Zacchini, P. Richards, *Coord. Chem. Rev.* **2002**, *227*, 193; c) G. M. Aspinall, M. C. Copsey, A. P. Leedham, C. A. Russell, *Coord. Chem. Rev.* **2002**, *227*, 217.

[17] However, it was demonstrated recently that both $P(OH)_3$ and $HP(OH)_2$ can be trapped and stabilized through coordination to a transition-metal center. $P(OH)_3$: M. N. Sokolov, A. V. Virovets, D. N. Dybtsev, E. V. Chubarova, V. P. Fedin, D. Fenske, *Inorg. Chem.* **2001**, *40*, 4816; $HP(OH)_2$: M. N. Sokolov, R. Hernández-Molina, W. Clegg, V. P. Fedin, A. Mederos, *Chem. Commun.* **2003**, 140**.**

[18] It took 10 days to optimize the geometries of **A** ($AlMe_3$) and **B** ($AlMe_3$) at the MP2/TZVPP level using a parallel version of Turbomole on a dual processor computer with 2000 MHz Intel Xeon CPUs and 2 GB of main memory. Since MP2 calculations scale with N^4 (N = number of atoms) the exchange of Me for *t*Bu and thus adding an extra 27 atoms is computationally prohibitive.

[19] G. E. Coates, K. Wade, *Organometallic Compounds, The Main Group Elements*, Methuen, London, **1967**.

[20] F. W. Reier, P. Wolfram, H. Schumann, *J. Cryst. Growth* **1988**, *93*, 41.

[21] H. Lehmkuhl, O. Olbrysch, H. Nehl, *Liebigs Ann. Chem.* **1973**, 708.

[22] R. A. Kovar, G. Loaris, H. Derr, J. O. Callaway, *Inorg. Chem.* **1974**, *13*, 1476.

[23] SHELXS-97, G. M. Sheldrick, *Acta Crystallogr. Sect. A* **1990**, *46*, 467.

[24] SHELXL-97, Program for Crystal Structure Refinement, G. M. Sheldrick, Universität Göttingen, 1997.

[25] TURBOMOLE, Version 5: a) R. Ahlrichs, M. Bär, M. Häser, H. Horn, C. Kölmel, *Chem. Phys. Lett.Chem. Phys. Letters* **1989**, *162*, 165; b) M. v. Arnim, R. Ahlrichs, *J. Chem. Phys.* **1999**, *111*, 9183; c) O. Treutler, R. Ahlrichs, *J. Chem. Phys.* **1995**, *102*, 346; d) current version: http://www.chemie.uni-karlsruhe.de/PC/TheoChem.

[26] a) K. Eichkorn, F. Weigend, M. Häser, R. Ahlrichs, *Theor. Chim. Acta* **1997**, *97*, 331; b) K. Eichkorn, O. Treutler, H. Ohm, M. Häser, R. Ahlrichs, *Chem. Phys. Lett.* **1995**, *242*, 652; c) J. P. Perdew, *Phys. Rev. B* **1986**, *33*, 8822; d) A. D. Becke, *Phys. Rev. A* **1988**, *38*, 3098; e) S. H. Vosko, L. Wilk, M. Nusair, *J. Can. Phys.* **1980**, *58*, 1200.

[27] A. Schäfer, H. Horn, R. Ahlrichs, *J. Chem. Phys.* **1992**, *97*, 2571.

[28] K. Eichkorn, F. Weigend, O. Treutler, R. Ahlrichs, *Theor. Chem. Acc.* **1997**, *97*, 119.

[29] P. Deglmann, F. Furche, R. Ahlrichs, *Chem. Phys. Lett.* **2002**, *362(5*,6), 511.

[30] F. Weigend, M. Häser, *Theor. Chem. Acc.* **1997**, *97*, 331.

[31] F. Weigend, M. Häser, H. Patzelt, R. Ahlrichs, *Chem. Phys. Lett.* **1998**, *294*, 143.

Received: September 10, 2003 [F5530]